Interchain Pressure Effect in Extensional Flows of Entangled Polymer Melts

Giuseppe Marrucci* and Giovanni Iannirubertо

Dipartimento di Ingegneria Chimica, Università Federico II, Piazzale Tecchio, 80125 Napoli, Italy

Received October 6, 2003; Revised Manuscript Received March 5, 2004

ABSTRACT: Recent data by Hassager and co-workers [Bach et al. *Macromolecules* **2003**, *36*, 5174] of elongational viscosity of nearly monodisperse polystyrene melts are interpreted by including in the classical tube theories for entangled polymer dynamics an interchain repulsive contribution. The proposed theory predicts the observed power law of η_{el} vs $\dot{\epsilon}$ in a straightforward way and qualitatively explains the observed scaling with the polymer molecular mass. Possible generalizations are discussed.

1. Introduction

The complex rheological behavior of entangled polymeric liquids has been investigated for many decades, both experimentally and theoretically. In recent times, however, what might perhaps be called a "standard model" has gained a diffused consensus, at least for the most common case of linear (as opposed to branched) polymer chains.

Such a standard description can be summarized as follows. The basis is the now well-known tube model of Doi and Edwards,[1] which includes the following items: (i) the tube (representing the constraints exerted on a given chain by the surrounding ones), the axis of which deforms affinely with the continuum, while the diameter stays constant; (ii) an instantaneous retraction of the chain within the tube so as to maintain a constant tube length; (iii) a relaxation (randomization) of the tube conformation through the 1D diffusion of the chain out of the old tube, a process named reptation by de Gennes.[2] In the Doi−Edwards model the chain tension has a constant value of $3kT/a$, where kT is thermal energy and a is tube diameter (the entanglement mesh size). The stress tensor is calculated from the ensemble average $\langle \mathbf{FR} \rangle$, where $\mathbf{R}$ is the end-to-end vector of a tube segment and $\mathbf{F}$ is the traction force in the corresponding subchain. Since $F = 3kT/a$ is a constant in the basic model, stress is due only to the flow-induced orientational anisotropy of tube segments.

Improvements of the basic model are best described by distinguishing contributions affecting viscoelasticity in general from those only relevant to the nonlinear response. To the first category belong (i) chain-end fluctuations,[3] which among other things explain the observed 3.4 power law of the viscosity as opposed to the third power predicted by the bare reptation mechanism, and (ii) constraint release due to thermal motion of the surrounding chains[4] which is particularly important in polydisperse situations. Since these effects contribute additional relaxation, they reduce the stress with respect to the prediction of reptation only.

Mechanisms that become operative, or even dominant, in the nonlinear range (large and fast deformations or fast flows) are chain stretch[1,5] and convective constraint release (CCR).[6] Chain stretch increases the tension in the chain above the equilibrium value $3kT/a$ and hence increases the stress. However, chain stretch is due to friction of the chain retracting within its tube, and hence it is predicted to occur only when the velocity gradient of the flow exceeds the reciprocal Rouse time τ_R of the chain, i.e., in very fast flows. Conversely, CCR becomes operative as soon as the velocity gradient exceeds the reciprocal reptation (or tube disengagement) time τ_d, the ratio τ_d/τ_R being of the order of the number of entanglements per chain. Although CCR is an additional relaxation mechanism, it may work in the direction of increasing the stress. This happens specifically in shear flows, where tube alignment in the shear direction at shear rates above the reciprocal reptation time (i.e., when reptation is effectively frozen) would cause the shear stress to approach zero; CCR prevents this to occur as it contributes to tube randomization in proportion to the shear rate itself, hence maintaining the shear stress at a plateau value.[7]

Models that include both CCR and chain stretch were progressively developed[8−12] and successfully compared with several data in the nonlinear range. Agreement has been deemed sufficiently satisfactory as to consider the standard model virtually definitive.[12] To complete our summary, however, it must be mentioned that an aspect of the standard model has been frequently challenged, namely the constant tube diameter. It has been repeatedly suggested that tube diameter and distance between entanglements should be affected by deformation,[13−17] and recently a systematic analysis of the tube behavior in entangled rubbers has been carried out.[18] There is a growing consensus that tube diameter effects should be somehow accounted for also in entangled polymeric liquids.[12]

In this paper we start from the recent experiments of elongational flow performed by Bach et al.[19] that, in our opinion, reveal a nontrivial crisis of the standard model. In the next section we review these findings, showing that the concepts generally accepted prove unable to explain those observations. Then, in the following sections we propose a possible interpretation based on a simple way of accounting for tube diameter change that appears physically sensible. A final discussion and perspectives of future work conclude the paper.

2. Elongational Viscosity

Before reviewing the data for monodisperse melts reported by Bach et al.,[19] let us recall what the standard

* Corresponding author: e-mail marrucci@unina.it.

10.1021/ma035501u CCC: $27.50
Published on Web 04/15/2004

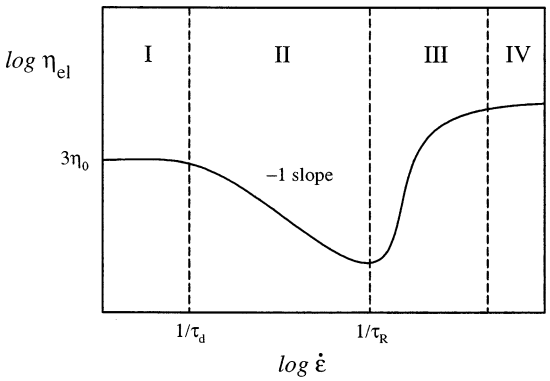

Figure 1. Steady-state elongational viscosity vs elongation rate $\dot{\epsilon}$ as predicted by standard molecular theories of entangled polymers. From the Trouton value $3\eta_0$ at low $\dot{\epsilon}$, the viscosity first decreases as $1/\dot{\epsilon}$ and then increases again when chains stretch out.

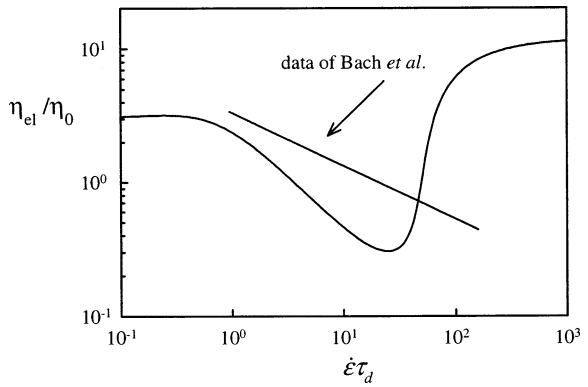

Figure 2. Same as in Figure 1 together with data of Bach et al., showing that the standard theory does not seem to apply to polymer melts.

model would predict for the elongational viscosity η_{el} in steady uniaxial elongational flow of a monodisperse polymer. Figure 1 shows schematically this prediction in the form of a logarithmic plot of η_{el} vs the stretching rate $\dot{\epsilon}$.

At low values of $\dot{\epsilon}$, i.e., as long as $\dot{\epsilon}$ remains smaller than τ_d^{-1}, the polymeric liquid maintains the equilibrium structure, and the viscosity is constant at the Trouton value (region I in Figure 1). When $\dot{\epsilon}$ becomes larger than τ_d^{-1} (yet smaller than τ_R^{-1}), reptation is effectively frozen, and tubes orient parallel to the elongation direction. Because chains are not stretched, and therefore carry the equilibrium tension $3kT/a$, the stress saturates together with the orientation of the tubes. For a full orientation of the tubes, the normal stress difference in the elongation direction becomes $\sigma = 3\nu kTL/a$, where ν is the number of chains per unit volume and L is the tube length. Then, since σ is a constant in this range of $\dot{\epsilon}$, the elongational viscosity $\eta_{el} = \sigma/\dot{\epsilon}$ scales as $\dot{\epsilon}^{-1}$ (region II in Figure 1). Notice that, although CCR makes the tubes to fluctuate about the elongation direction (somewhat reducing the stress from the value $\sigma = 3\nu kTL/a$), still σ is predicted to remain constant in this region and hence η_{el} to scale as $\dot{\epsilon}^{-1}$. Finally, when $\dot{\epsilon}$ is comparable to (or larger than) the reciprocal Rouse time τ_R^{-1}, chains stretch out, and this behavior results in an upturn of η_{el} (region III in Figure 1). The elongational viscosity ultimately saturates when the chains become fully stretched (region IV).

The scaling of the relevant quantities in Figure 1 with the molecular mass M of the polymer is as follows. The equilibrium Trouton value of η_{el}, as well as the reptation time τ_d, scales as $M^{3.4}$. The constant value of σ in region II is independent of M, just like the plateau modulus. Indeed, $3\nu kTL/a$ differs from the plateau modulus only by a numerical factor. As is well-known, the Rouse time τ_R scales like M^2. Finally, the value of η_{el} corresponding to fully stretched chains also scales like M^2, and hence it can be larger or smaller than the Trouton value, depending on M.

Predictions of the standard model as depicted in Figure 1 have been recently compared with data of entangled polymeric solutions, and a generic good agreement has been found.[20−22] Indeed, the steady-state viscosity shows a nonmonotonic behavior as predicted in Figure 1; i.e., it first decreases with increasing $\dot{\epsilon}$ and then goes through a minimum to increase again after that. Moreover, the location of the minimum seems consistent with the estimate for the Rouse time.[20,21] However, in view of the considerations developed in the next sections, it seems important to report a sentence of the Conclusions section of the paper by Bhattacharjee et al.[20] whereby, after comparing polystyrene solution data to various detailed models (variants of the standard model), the authors conclude: "Specifically, the steady state predictions for the extensional viscosity are lower than the data in all cases, and are lower by large amounts depending on the strain rate that is chosen".

In the case of molten polymers (as opposed to solutions), the experimental determination of steady-state values of the elongational viscosity is a more difficult task, and the few values reported in past years were typically obtained for commercially relevant, polydisperse polymers and hence difficult to compare with theory. The recent data of Bach et al.[19] seem to constitute the first results that can be used unequivocally. While referring to the original reference for all details, we here discuss the main aspects of those results. The new curve in Figure 2 (new with respect to Figure 1) is a schematic representation of one set of data obtained by Bach et al. (polystyrene of mass 200K, reported in their Figure 6).

Two aspects of these data are worth of note. The first of them is that, although η_{el} appears to depart from the Trouton value at the right place ($\dot{\epsilon} \approx \tau_d^{-1}$), it then decreases approximately as $\dot{\epsilon}^{-1/2}$ (instead of $\dot{\epsilon}^{-1}$) for more than 2 decades in $\dot{\epsilon}$. The second aspect is that the data seem to go well beyond $\dot{\epsilon} = \tau_R^{-1}$ without showing any sign of an upturn. Departure from the prediction of the standard model could not be more dramatic. Region II has a drastically different behavior (slope $-1/2$ instead of -1), and regions III and IV do not seem to be reached.

The second set of data of Bach et al. (polystyrene of mass 390K) show a similar behavior, confirming the vast discrepancy. Moreover, the stress σ in region II (which in the standard model is a constant independent of M) is actually found to depend on M. Bach et al. show that the two sets of data (PS 200K and 390K) collapse into a single line if σ/M is plotted vs $\dot{\epsilon}$ or, equivalently (in view of the $1/2$ slope), if σ is plotted vs $\dot{\epsilon}M^2$ or vs $\dot{\epsilon}\tau_R$.

The apparent crisis of the standard model is recognized by Bach et al. themselves, who note in the Discussion section of their paper that the stress "is well above ... the maximum stress obtained by orientation according to the basic DE model", taking this as "... a signature of substantial chain stretching". Yet such an apparent stretching starts in region II well below the reciprocal Rouse time, generating a stress that grows

with a mysterious one-half power law of $\dot{\epsilon}$, and continues into region III with "... no sign of changes in qualitative behavior when the nondimensional elongation rate ($\dot{\epsilon}\tau_R$) is of order unity".

Although the data of Bach et al. are the first of their kind, and future confirmations are certainly welcome, we tend to believe that they cannot be treated as mere accidents. The observed simple scaling of stress with both $\dot{\epsilon}$ and M in region II is strongly suggestive that some new physical effect is dominant in that range. In the next sections, we advance a suggestion on what such a physical ingredient could be.

3. Pressure of the Chain in the Tube

It is commonly accepted that polymer chains develop traction forces of thermal origin when they are constrained. Thus, it is well-known that if an ideal chain is fixed at the ends, at a distance R, the force is given by $F = (3kT/nb^2)R$, where n and b are the number and length, respectively, of the Kuhn segments forming the chain. The equilibrium traction force of the chain in the tube, $F = 3kT/a$, is but a special application of the same formula for $nb^2 = a^2$ and $R = a$.

However, chains confined in a box also exert a thermal pressure on the confining wall. If the box dimension in the x-direction, say, is smaller than the chain size, then the pressure exerted by the chain on the wall orthogonal to the x-direction is given by[23]

$$p_x = \frac{\pi^2}{3}\frac{Nb^2}{L_x^2}\frac{kT}{V} \tag{1}$$

where N is the total number of monomers in the chain, L_x is the box dimension along x and V is the box volume.

Let us consider the tubes of the entangled system in the range of $\dot{\epsilon}$ values corresponding to region II in Figure 1. Because reptation is suppressed, the tubes are nearly parallel to the stretching direction (z-axis, say). Hence, in the z-direction there is the classical chain traction $3kT/a$. However, by using eq 1, with $L_x \approx a$ and $V \approx a^2L$ (where L is tube length), we also calculate a thermal pressure exerted on the "tube wall" in the x and y directions, given by

$$p \approx kT\frac{Nb^2}{a^4L} \tag{2}$$

(Here and in the following the symbol $\approx$ indicates that numerical coefficients of order unity are ignored.) Multiplication of p to the lateral surface area of the tube, aL, gives the overall compressive force F exerted by the chain in the x and y directions:

$$F \approx kT\frac{Nb^2}{a^3} \tag{3}$$

The force F is interpreted as acting against the topological constraints of the chain (the "tube wall") and will be used in the next section to develop a dynamical equation for the tube diameter a. Here it is used to calculate the macroscopic normal stress components in the x and y directions, given by

$$\sigma_{xx} = \sigma_{yy} \approx -\nu kT\frac{Nb^2}{a^2} \tag{4}$$

where ν is the number of chains per unit volume and the negative sign indicates compression. Equation 4 is obtained from eq 3 in the classical way, i.e., by considering that (since all tubes are aligned in the z-direction) a cut orthogonal to the x (or y) direction will intercept all chains contained in a slab of thickness a (and none outside), hence, per unit area of the cut, a number of chains equal to νa, all of them exerting the force F of eq 3.

Similarly, since in the z-direction all tubes are of length L, and all chains carry the same traction of order kT/a, one obtains

$$\sigma_{zz} \approx \nu L\frac{kT}{a} \approx \nu kT\frac{Nb^2}{a^2} \tag{5}$$

where the latter equality assumes that the chain remains equilibrated within the tube and hence that the linear monomer density remains proportional to the tube diameter ($N/L = a/b^2$).[1]

Except for the sign, eqs 4 and 5 are the same expression (but compare the Appendix for numerical coefficients, here ignored, that become important when comparing different elongational flows). Hence, the relevant normal stress difference can also be written as

$$\sigma = \sigma_{zz} - \sigma_{xx} \approx \nu kT\frac{Nb^2}{a^2} \tag{6}$$

In this expression for the elongational stress, all quantities remain constant during flow, with the possible exception of the tube diameter a. Indeed, the expression in eq 6 was used previously by others, notably by Wagner and co-workers,[15,16] who have considered a variable tube diameter. In the next section, we examine how the tube diameter a can sensibly be expected to vary from its equilibrium value a_0, as a function of the stretching rate $\dot{\epsilon}$ in region II.

4. Dynamical Equation

Should the wall of a tube move affinely with the imposed deformation, which preserves the volume, the rate of change of the tube diameter a would be (tubes in region II are essentially aligned to the stretching direction):

$$\dot{a}_{\text{affine}} = -\frac{\dot{\epsilon}}{2}a \tag{7}$$

Because of CCR, which continuously removes obstacles in proportion with $\dot{\epsilon}$, the rate of change of a (inclusive of CCR effects) will in fact be

$$\dot{a}_{\text{convective}} = -\beta\dot{\epsilon}a \tag{8}$$

where β is a positive numerical factor, not quite known, but certainly smaller than 0.5 as CCR works in the direction of opposing the affine contraction of the tube. The more effective is CCR, the closer to zero is β. We tend to exclude a zero value of β, however, both because it implies that CCR completely cancels the affine contraction, which seems exaggerate, and also because otherwise a remains constant at the equilibrium value a_0, and we are back to the standard model with no hope of explaining the experimental evidence.

No matter what value has β (as long as it is not zero), eq 8 would predict that the tube diameter a decreases indefinitely. Conversely, the data of Bach et al.[19] show that a steady state is reached, which varies with $\dot{\epsilon}$. Hence, we argue in the following way.

While a decreases, pressure builds up against the tube wall as described in the previous section. Such a growing pressure will eventually stop the contraction process. When steady state is reached, a force balance may be written as

$$kTNb^2\left(\frac{1}{a^3}-\frac{1}{{a_0}^3}\right)\approx\zeta|\dot{a}_{\text{convective}}|\approx\zeta\dot{\epsilon}a \tag{9}$$

where we have used eq 3 for the compressive force on the tube wall, and ζ is a suitable friction coefficient of the chain to be discussed below. In the last approximate equality we have included β in the unknown numerical coefficient of order unity. The left-hand side of eq 9 is written as a difference between the existing compressive force and that at equilibrium so as to obtain $a = a_0$ for a vanishing $\dot{\epsilon}$. However, as a decreases from the equilibrium value, the term containing a_0 soon becomes negligible, and eq 9 reduces to the power law:

$$a\approx\left(\frac{kTNb^2}{\zeta\dot{\epsilon}}\right)^{1/4} \tag{10}$$

It is remarkable that a simple balance between the pressure force F of eq 3 and a friction force of the form $\zeta\dot{a}$ provides such a major result, i.e., the prediction that a should scale as $\dot{\epsilon}^{-1/4}$ in steady-state elongational flow. Indeed, if we replace eq 10 into eq 6, we obtain for the normal stress difference

$$\sigma\approx\nu(kTNb^2\zeta\dot{\epsilon})^{1/2} \tag{11}$$

and the predicted scaling of σ with $\dot{\epsilon}^{1/2}$ is in full agreement with the experiments of Bach et al.

The dependence of σ on the polymer molecular mass M embodied in eq 11 is now examined. The friction coefficient ζ of the chain introduced in eq 9 is expected to be additive over the monomers of the test chain, so that by considering the friction per monomer (or per Kuhn segment)

$$\zeta_{\text{m}}=\zeta/N \tag{12}$$

eq 11 is rewritten as

$$\sigma\approx\nu N(kTb^2\zeta_{\text{m}}\dot{\epsilon})^{1/2}=\nu_{\text{m}}(kTb^2\zeta_{\text{m}}\dot{\epsilon})^{1/2} \tag{13}$$

where $\nu_{\text{m}} = \nu N$ is the number of monomers per unit volume of the melt, which is independent of M.

The only quantity in the last expression for σ that possibly depends on M is therefore ζ_{m}. In fact, though defined for a single monomer of the test chain, ζ_{m} is not an ordinary monomeric friction coefficient: ζ_{m} refers to the *effective* friction encountered in pushing back the surrounding chains that are squeezing the test chain, and it seems reasonable to expect that ζ_{m} does depend on the length of the surrounding chains.

To find an expression for ζ_{m}, we argue as follows. Let us consider a blob of the test chain of size l (to be identified below) containing n monomers ($n = l^2/b^2$). The "lateral" diffusion coefficient of this blob is then given by $D_{\text{b}} = kT/n\zeta_{\text{m}} = kTb^2/l^2\zeta_{\text{m}}$, while the ratio l^2/D_{b} gives the time required for the blob to diffuse a distance l into the surroundings. On the other hand, in order that the surrounding chains permanently accommodate the disturbance created by the diffusion step considered (rather than elastically pushing the blob back), a time of the order of the Rouse time τ_{R} of the surrounding chains must necessarily elapse. We then equate l^2/D_{b} to τ_{R}, and we obtain for the unknown friction coefficient ζ_{m}:

$$\zeta_{\text{m}}\approx\frac{kTb^2}{l^4}\tau_{\text{R}} \tag{14}$$

Equation 14 in fact relates ζ_{m} to a similarly unknown quantity l. Progress has been achieved, however, insofar as l is independent of M, and hence the dependence of ζ_{m} on molecular mass is identified with that of τ_{R}. Indeed, we interpret l as the characteristic size of local fluctuations of the tube diameter, which obviously is independent of M. As mentioned above, such fast fluctuations are elastically localized, but only up to times of order τ_{R}, when the retracting motion of the surrounding chains can accommodate them, and let them diffuse.

By using eq 14, the expression for stress of eq 13 is rewritten as

$$\sigma\approx\nu_{\text{m}}kT\frac{b^2}{l^2}(\tau_{\text{R}}\dot{\epsilon})^{1/2} \tag{15}$$

which fully reproduces the scaling of σ with M observed by Bach et al. We admit that the argument is not completely satisfactory, specifically because we do not precisely know how to calculate the new length l, but at the moment we are unable to offer anything better. We expect of course that l falls within the interval $b < l < a_0$. In fact, on the basis of general fluctuation theory, we would suggest $l \approx \sqrt{ba_0}$.

In considering eq 15, one should note that, although in region II $\tau_{\text{R}}\dot{\epsilon}$ is less (possibly much less) than unity, it is quite conceivable that σ comes out greater than the plateau value of the classical theory, as indeed observed by Bach et al. To prove this, let us rewrite the "modulus" in front of the square root term of eq 15 as (L_0 is the equilibrium value of L):

$$\nu_{\text{m}}kT\frac{b^2}{l^2}=\nu kT\frac{Nb^2}{l^2}=\nu kT\frac{L_0a_0}{l^2}=\left(\frac{{a_0}^2}{l^2}\right)\left(\nu kT\frac{L_0}{a_0}\right)\approx\frac{{a_0}^2}{l^2}\sigma_{\text{plateau}} \tag{16}$$

In the last expression of eq 16, σ_{plateau} indicates the plateau value predicted by the standard model in region II. On the other hand, the factor a_0^2/l^2 in front of it is certainly larger (possibly much larger) than unity.

We now return to the dynamical equation, eq 9, to rewrite it for a transient case. For the rate of change of the tube diameter we would write

$$\frac{\text{d}a}{\text{d}t}=-\dot{\epsilon}a+\frac{kTNb^2}{\zeta}\left(\frac{1}{a^3}-\frac{1}{{a_0}^3}\right) \tag{17}$$

The first term on the right-hand side of eq 17 is the convective forcing term of eq 8 (without the β factor for simplicity), while the second term describes relaxation toward equilibrium driven by the compression force. To extract the characteristic relaxation time of this process,

we make use of eqs 12 and 14 for ζ and rewrite eq 17 as

$$\frac{da}{dt} = -\dot{\epsilon}a + \frac{a_0}{\tau_p}\left(\frac{a_0^3}{a^3} - 1\right) \tag{18}$$

where

$$\tau_p = \frac{a_0^4}{l^4}\tau_R \tag{19}$$

Therefore, τ_p represents the relaxation time of the squeezing pressure effect. Notice that, although τ_p scales with M just like the Rouse time of the chain, it does not coincide with τ_R and is in fact larger by the factor a_0^4/l^4. Hence, the condition $\dot{\epsilon}\tau_p \approx 1$, determining the onset of the squeezing effect, is reached at a much lower stretching rate than $\dot{\epsilon}\tau_R \approx 1$, representing the onset of chain stretching.

Since the squeezing relaxation time is larger than the Rouse time, it may well be comparable with the reptation time. However, because the two times scale differently with the molecular mass, the relation between them changes with M. We expect $\tau_p > \tau_d$ for less entangled polymers and the opposite situation at high M.

Before examining the two cases in some detail, we need to complete the dynamical equation for the tube diameter, eq 18. Indeed, we have so far ignored that the chain has an escape possibility, alternative to that of pushing back the surrounding material. That is, if the chain reptates out of the squeezed tube fast enough, the equilibrium diameter a_0 (created by the chain ends) is restored. Hence, the dynamical equation for a is completed by writing

$$\frac{da}{dt} = -\dot{\epsilon}a + \frac{a_0}{\tau_p}\left(\frac{a_0^3}{a^3} - 1\right) + \frac{a_0 - a}{\tau_d} \tag{20}$$

where the last term implies (should it prevail) an exponential relaxation of a toward a_0 with the reptation time τ_d, as it should. (Higher reptation modes and chain end fluctuations are ignored.)

Here we only consider the steady-state situation, described by the algebraic equation (replacing eq 9)

$$\frac{a_0}{\tau_p}\left(\frac{a_0^3}{a^3} - 1\right) + \frac{a_0 - a}{\tau_d} = \dot{\epsilon}a \tag{21}$$

which defines the function $a/a_0 = f(\dot{\epsilon}\tau_p, \tau_d/\tau_p)$. This function is plotted in Figure 3 for several values of the ratio τ_d/τ_p, both below and above unity. In all cases the function gives $a = a_0$ for small $\dot{\epsilon}$, while at high $\dot{\epsilon}$ it reduces to the power law

$$a/a_0 = (\dot{\epsilon}\tau_p)^{-1/4} \tag{22}$$

which is the same of eq 10. The transition region, however, is sensitive to the ratio τ_d/τ_p, as the departure of a from the equilibrium value only occurs when $\dot{\epsilon}$ reaches the *largest* of the two reciprocal times τ_d^{-1} or τ_p^{-1}. Hence, at high M where τ_p controls, the curve in Figure 3 becomes independent of M, whereas at low M where reptation is faster, the transition zone explicitly depends on M.

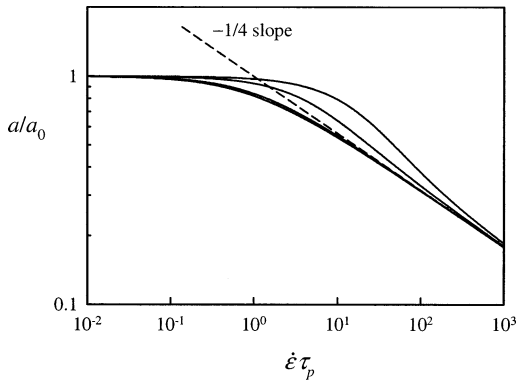

Figure 3. Tube diameter vs elongation rate as predicted by eq 21. The broken line is the power law of eq 22. Parameter of the curves is $\tau_d/\tau_p = 0.03$, 0.1, 1, and 10 from top to bottom. The curve for $\tau_d/\tau_p = 10$ virtually coincides with the universal curve at high M.

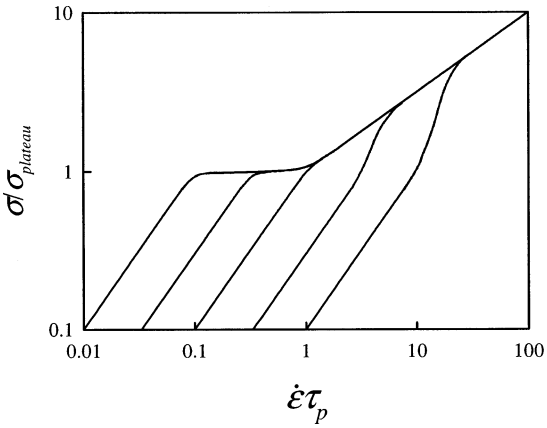

Figure 4. Nondimensional stress vs $\dot{\epsilon}\tau_p$ for several values of the ratio $\tau_d/\tau_p \propto M^{1.4}$. From left to right $\tau_d/\tau_p = 10$, 3, 1, 0.3, and 0.1. Tubes become oriented at $\dot{\epsilon}\tau_d \cong 1$, i.e., at $\sigma/\sigma_{plateau} \cong 1$. Although the linear region, the plateau, and the power law of eq 23 are quantitative, the transition regions between them are drawn schematically.

The corresponding diagram for the elongational stress σ (made nondimensional by taking the ratio to $\sigma_{plateau}$) is sketched in Figure 4. At low stretching rates, the elongational stress is proportional to $\dot{\epsilon}$ through the Trouton viscosity. On the other hand, at high $\dot{\epsilon}$, all curves converge to the power law:

$$\sigma/\sigma_{plateau} = (\dot{\epsilon}\tau_p)^{1/2} \tag{23}$$

The transition region then must show a quite reach behavior. Indeed, two physical transitions should be considered: i.e., the orientational transition that always occurs at $\dot{\epsilon} \approx \tau_d^{-1}$, when reptation is frozen and tubes become oriented to the elongation direction, and the tube diameter squeezing transition depicted in Figure 3.

The case $\tau_d > \tau_p$ (high M) is examined first. For such a situation, the two transitions occur separately. At $\dot{\epsilon} \approx \tau_d^{-1}$ tubes become oriented, but their diameter stays at the equilibrium value. Hence, the linear behavior of σ controlled by the Trouton viscosity starts yielding to the plateau value predicted by the standard model for region II. Only when $\dot{\epsilon}$ increases up to the value of τ_p^{-1} is the transition to the power-law regime of eq 23 approached. (See curves to the left in Figure 4, approaching the asymptotic straight line of eq 23 from above.)

Conversely, for $\tau_d < \tau_p$ (low M), the two transitions occur simultaneously. When $\dot{\epsilon} \approx \tau_d^{-1}$ (always corresponding to $\sigma \approx \sigma_{plateau}$), tubes become oriented to the elongation direction. At the same stretching rate, however, since $\dot{\epsilon}$ already is larger than τ_p^{-1}, the tube diameter a immediately starts to decrease toward the power law of eq 22. Correspondingly, σ starts approaching eq 23. (See curves to the right in Figure 4, approaching the asymptote from below.) Notice that, in this case, it cannot be excluded that the viscosity raises *above* the Trouton value in the transition region.

Finally, for $\tau_d \approx \tau_p$, the linear regime is expected to yield immediately to the power law of eq 23. (See middle curve in Figure 4.) We tend to believe that the PS 200K data of Bach et al. fall close to the latter situation, while the PS 390K data correspondingly fall under the case $\tau_d > \tau_p$, for which the $^1/_2$ power law is approached from above. (Compare our Figure 4 with Figure 7 of their paper.)

5. Quantitative Comparison with the Data of Bach et al.

We here perform a quantitative comparison with the data of Bach et al.[19] More precisely, since all equations describing the new effect ignore numerical coefficients of order unity, the comparison is in fact semiquantitative. The first step will be that of estimating the unknown new time τ_p by fitting the $^1/_2$ power law of eq 23 to the data of Bach et al.

Let us consider the PS200K sample first, for which Figure 7 of Bach et al. reports the ratio σ/G_N^0 of the normal stress difference to the plateau modulus as a function of the stretching rate $\dot{\epsilon}$. Since $\sigma_{plateau}$ and G_N^0 are of comparable magnitude, eq 23 identifies τ_p with the reciprocal of $\dot{\epsilon}$ for which σ/G_N^0 is nearly unity. From Figure 7 of Bach et al., we then estimate (at 130 °C)

$$\tau_p(200K) \approx 10^3 \text{ s}; \quad \tau_p(390K) \approx 3.4 \times 10^3 \text{ s}$$

where the second result is obtained by scaling with M^2.

We now compare the estimated values of τ_p for the two polymers with the corresponding reptation times, reported by Bach et al. These are

$$\tau_d(200K) \cong 1040 \text{ s}; \quad \tau_d(390K) \cong 11.300 \text{ s}$$

Notice that, for the 200K sample, it is $\tau_d \approx \tau_p$, and correspondingly, it is $\tau_d \gg \tau_p$ for the 390K sample. Hence, by recalling the discussion at the end of the previous section on the transition toward the power law, we find good agreement of the theoretical prediction with the behavior shown by the data in Figures 6 and 7 of Bach et al. Indeed, PS200K appears to obey the power law from the very start, while PS390K shows a transition region in which the power law is approached from above.

To proceed, we now need to estimate the Rouse time of these polymers (not reported in the paper by Bach et al.). We use the concept that, by extrapolating the zero-shear viscosity from the entangled region down to the critical molecular mass M_c, such extrapolated value also obeys the Rouse theory, as is typical of low-M melts. The zero-shear viscosities (at 130 °C) of PS200K and PS390K are 84 and 755 MPa s, respectively, and scale with M to the power 3.3.[19] Hence, since $M_c \cong 35\,000$,[24,25] we extrapolate a value of $\eta_0(M_c) \cong 0.27$ MPa s. Then using the Rouse relationship $\tau_R = (6/\pi^2)\eta_0/\nu kT$,[25] we estimate $\tau_R(M_c) \cong 1.7$ s. Finally, by scaling with M^2, we obtain

$$\tau_R(200K) \cong 50 \text{ s}; \quad \tau_R(390K) \cong 200 \text{ s}$$

We now examine the problem of the chain stretch that should take place when $\dot{\epsilon}$ becomes larger than τ_R^{-1}. According to the estimated values of the Rouse time, chain stretch should begin around $\dot{\epsilon} \cong 0.02$ s^{-1} for the 200K polymer and around $\dot{\epsilon} \cong 0.005$ s^{-1} for the 390K. On the other hand, the data of Bach et al. extend up to nearly 10 times as much for the 200K polymer (and even 20 times for the 390K) without showing any upward departure from the $^1/_2$ power law. In the next section, we discuss the possibility that the Rouse time as reported above is overestimated.

We conclude here by estimating the unknown length l. From the values of τ_R and τ_p reported above, eq 19 gives

$$l^4/a_0^4 \cong 0.05; \quad l/a_0 \cong 0.5$$

Needless to say, if really τ_R is overestimated, then l is in fact smaller than reported above.

6. Discussion

The first point to be considered is the reason why the data of Bach et al. do not show any upturn due to chain stretching, although the data apparently extend up to values of $\dot{\epsilon}\tau_R$ of order 10. As already mentioned in the previous section, we suspect that τ_R is overestimated. Indeed, we have calculated τ_R on the basis of the classical assumption whereby the extrapolated viscosity at M_c obeys the Rouse theory. On the other hand, there exists an ever growing evidence that appears to disprove the assumption.[26−30] The recent molecular dynamics simulations of Padding and Briels[30] very clearly show that the Rouse behavior holds only up to a value of M that is significantly smaller than the entanglement molecular mass M_e and hence much smaller than the critical mass M_c. An intermediate regime is found by them, in which the melt viscosity scales with $M^{1.8}$. From the same results, one estimates (cf. Figure 19 of Padding and Briels[30]) that the melt viscosity at M_c is about 5 times larger than the extrapolated Rouse value. This would imply that the classical assumption overestimates τ_R by roughly the same factor.

Leaving aside simulations, and considering real data, it is recalled that the low-M data (collected at constant temperature and pressure) are not isofrictional, and require a free volume correction. After the correction is made, the low-M data appear to follow the Rouse theory virtually up to M_c.[24,31] However, a detailed description of how the correction is accomplished[31] shows that an assumption is in fact required and that some consequences of the assumption are not satisfactory. Admittedly,[31] the values and trends of some characteristic parameters come out much different from normal expectations. It so appears that the correction generating the Rouse-like behavior of the low-M melts contains serious uncertainties. On the other hand, older data of linear viscoelasticity for low-M polystyrene melts[32] explicitly show that the Rouse theory is not fully obeyed. More specifically, in the ω range where Rouse theory predicts that G' and G'' should superimpose on one another and grow with $\omega^{1/2}$, the data do show a growth of G' and G'' roughly with $\omega^{1/2}$, but G' and G'' do not

superimpose. For $M = 10200$, i.e. close to M_e, G'' in fact runs higher than G' by a factor of ca. 3, thus revealing a much higher effective friction.

In conclusion, the hypothesis that the Rouse time of the polystyrene melts is in fact significantly smaller than estimated in the previous section does not appear implausible, and this might help explaining why the data of Bach et al., contrary to those of Bhattacharjee et al.[20,21] and of Ye et al.[22] for polystyrene solutions, do not show any upturn throughout the range of stretching rates explored.

We now discuss the main hypothesis advanced in this paper, i.e., the existence of the squeezing pressure effect generating the $^1/_2$ power law regime. In many off-lattice simulations of polymer melts, where the uncrossability constraint is enforced through suitable repulsive potentials, interchain contributions to the stress tensor come out comparable in magnitude to intrachain contributions arising from the chain connectivity.[33,34] We believe that this finding can be translated into the ideas developed in this paper: indeed, intrachain connectivity generates the classical chain traction, whereas interchain repulsive interactions correspond to the pressure effect. It is not clear, however, whether the pressure effect here proposed also is relevant for the case of entangled solutions. The existing elongational data for solutions[20−22] are ambiguous in this regard, as they have a rather short region II; i.e., reptation and Rouse times are close to one another (cf. Figure 1), and therefore a definite power law regime can hardly be observed. The existing solution viscosity data in region II do not obey the -1 power law predicted by the standard model and, as emphasized in section 2, are in fact significantly higher.[20] Whether this discrepancy is an indication of the $^1/_2$ slope regime similar to that of Bach et al. is hard to decide at this stage. On the other hand, even if additional evidence and a more detailed analysis should conclude that entangled solutions and melts do not behave exactly alike, this would not come to a complete surprise, as other aspects of polymer viscoelasticity also appear to discriminate between the two conditions.[35]

Another important point to be discussed is how the tube squeezing mechanism here proposed affects the stress response in flows other than the uniaxial extension so far considered. It is fair to note that uniaxial extension is the simplest case to be analyzed, especially in region II when tube are all aligned to the same direction. Already more complicated are other types of elongational flows (planar and biaxial) that, even when tubes are well oriented as in region II, do not enjoy the uniaxial symmetry. A comparison among different elongational flows is performed in the Appendix, where some of the numerical coefficients of order unity (ignored in the main text) are also accounted for. Predictions appear compatible with the limited experimental data available in the literature.

Needless to say, although the focus of this paper is on extensional flows, a very important test of the proposed mechanism is in the shear case. Here again the standard model is not fully satisfactory, as it predicts (in this case as well) that the non-Newtonian viscosity of monodisperse polymers decreases with increasing shear rate $\dot{\gamma}$ according to a power law with a -1 exponent, followed at higher shear rates by an upturn due to chain stretching. Data, on the other hand, can be fitted by a power law with a negative exponent of ca. $0.7-0.8$. Here again, the observed $\dot{\gamma}^{-0.7}$ or $\dot{\gamma}^{-0.8}$ power laws are usually interpreted as a pretransitional effect of chain stretching, while they might be indicative of the pressure effect.

However, shear flow predictions that account for the tube compression mechanism are not readily obtained, and work on shear flows is currently in progress. Indeed, contrary to the elongational case, for which tubes in region II are permanently aligned to the stretching directions (to within fluctuations due to CCR), individual tube orientation in a steady shear flow has a complex time dependence. Shear flow has a rotational component that makes chains to rotate continuously, even if macroscopically a steady-state average orientation is perceived. During rotation, tubes get alternatively squeezed and dilated; hence, average effects are not easily reckoned. Preliminary calculations indicate that in the nonlinear range a long transition takes place, lasting a few decades in $\dot{\gamma}$, in which the pressure effect makes the stress to increase progressively (yet very mildly) with $\dot{\gamma}$ over and above the CCR plateau, to approach only eventually a $^1/_2$ power law regime similar to that predicted here for elongational flows.

The complications of the shear case clearly indicate that a constitutive equation incorporating the tube squeezing effect is a premature goal. A further complication is that, once the idea is accepted that the tube diameter is not a constant, there is no reason to preserve in general the circular symmetry of the tube cross section. In other words, elliptical tubes must be considered,[36] as already done in the Appendix to deal with planar and biaxial elongational flows.

A final remark concerns the stress−optical law, which has often been tested experimentally and proved to remain valid well within the range of nonlinear viscoelasticity. The question might then arise whether the introduction of a pressure contribution to the stress tensor preserves the validity of the stress−optical law. In fact, we have already addressed this point, directly for the case of tubes with elliptical cross sections, showing that the stress−optical law remains fulfilled.[36]

7. Conclusions

We have shown that recent elongational viscosity data for entangled monodisperse polystyrene melts,[19] exhibiting a mysterious $^1/_2$ power law with the stretching rate $\dot{\epsilon}$, can be explained within the classical tube theories if the additional assumption is made that interchain repulsive interactions are present and that the latter are equivalent to a thermal pressure exerted by the chain against the tube wall. The expression used for that pressure is the classical one for a chain constrained in a box.[23]

A simple dynamical equation describing the change of tube diameter has been proposed, which only applies to the case where the elongational flow has essentially aligned the tubes to the stretching direction. From the analysis a new time constant τ_p comes out, which scales with the square of the polymer mass M but is larger than the Rouse time by the ratio a_0^4/l^4, where a_0 is the equilibrium diameter of the tube and l is a measure of tube diameter fluctuations. The dynamical equation readily predicts the $^1/_2$ power law for the stress and also describes the transition toward the power law (at least qualitatively). The observed scaling with M is also fully explained in terms of τ_p.

The evidence in favor of the interchain pressure effect here described is not limited to the data of Bach et al.[19] that, however, effectively stimulated the present work.

Indeed, it must be admitted that the stress plateau predicted by CCR in steady shear flows, as well as the elongational stress plateau of region II, is hardly observed in a strict sense in any system. In all cases, stress actually increases with deformation rate, more or less steeply. It is highly tempting to attribute the excess stress to the pressure effect. Also, Archer and co-workers repeatedly reported that relaxation after large step strains indicates the existence of an intermediate relaxation time between Rouse and reptation.[37,38] Of course, whether that indication actually relates to τ_p remains to be ascertained. Further theoretical work is obviously required and is in fact in progress. We also hope that further elongational viscosity data are collected for well-characterized polymer melts.

Acknowledgment. We are very grateful to Prof. Ole Hassager for sending us the manuscript of his paper prior to publication. We also thank the anonymous referees for their very useful comments that lead to improvements of this paper.

Appendix. Comparison of Uniaxial, Planar, and Equibiaxial Elongational Flows in Region II

The limited existing data on the various types of elongational flows of polymer melts (mostly by Meissner and co-workers[39,40]) seem to indicate that, at equal values of the stretching rate $\dot{\epsilon}$, the primary normal stress difference σ close to steady-state conditions is ordered as follows:

$$\sigma_{\text{uniaxial}} > \sigma_{\text{planar}} > \sigma_{\text{equibiaxial}} \tag{A1}$$

It appears important, therefore, to verify whether the ideas presented here predict such an ordering. This is the more challenging in the context of a theory emphasizing tube compression, as the matrices of the elongational kinematics are given by respectively

$$\underset{\textit{uniaxial}}{\begin{vmatrix} -\dot{\epsilon}/2 & 0 & 0 \\ 0 & -\dot{\epsilon}/2 & 0 \\ 0 & 0 & \dot{\epsilon} \end{vmatrix}} \quad \underset{\textit{planar}}{\begin{vmatrix} -\dot{\epsilon} & 0 & 0 \\ 0 & 0 & 0 \\ 0 & 0 & \dot{\epsilon} \end{vmatrix}} \quad \underset{\textit{equibiaxial}}{\begin{vmatrix} -2\dot{\epsilon} & 0 & 0 \\ 0 & \dot{\epsilon} & 0 \\ 0 & 0 & \dot{\epsilon} \end{vmatrix}} \tag{A2}$$

showing that the compressive effect (the negative elements of the matrices) is ordered in the opposite direction ($^1/_2 < 1 < 2$).

To proceed with the comparison, we need to detail some of the numerical factors of order unity that we have ignored so far. In view of the different symmetries of the various elongational flows, we are also forced to consider a complication that we could ignore in the uniaxial case. We have to expect that, in the general case, the tube cross section becomes elliptical. Specifically, in *planar* elongational flow, once the tubes are aligned to the stretching direction, we expect an elliptical cross section with the minor axis in the compression direction and the major axis (probably with the equilibrium size a_0) in the neutral direction. Similarly, in the so-called *equibiaxial* case, once the tubes are randomly oriented to all directions of the stretching plane, the tube cross section is expected to have the minor axis (smaller than a_0) in the compression direction, whereas the major axis (lying in the stretching plane) is probably even larger than a_0.

Tubes with elliptical cross sections were considered in a previous paper.[36] We rewrite here the expression for the stress tensor **T**, reported as eq 11 in that paper:

$$\mathbf{T} = \frac{1}{3}\nu_m kT\,[\langle -(la_y/2a_x\sqrt{a_x^2 + a_y^2})\hat{\mathbf{x}}\hat{\mathbf{x}} - (la_x/2a_y\sqrt{a_x^2 + a_y^2})\hat{\mathbf{y}}\hat{\mathbf{y}} + (l\sqrt{a_x^2 + a_y^2}/a_x a_y)\hat{\mathbf{z}}\hat{\mathbf{z}}\rangle]/[\langle la_x a_y/b^2\sqrt{a_x^2 + a_y^2}\rangle] \tag{A3}$$

Here, $\hat{\mathbf{x}}$, $\hat{\mathbf{y}}$, $\hat{\mathbf{z}}$ indicate a local set of orthonormal (unit) vectors, where $\hat{\mathbf{z}}$ is along the tube axis, while $\hat{\mathbf{x}}$ and $\hat{\mathbf{y}}$ lie along the axes of the elliptical cross section, a_x and a_y indicating the corresponding tube dimensions. Length l is that of the tube segment, and $\langle\cdots\rangle$ indicates ensemble average. In all cases considered here, however, a_x and a_y are constant in the ensemble, and also l can be taken as constant with no loss of generality. Hence, eq A3 simplifies to

$$\mathbf{T} = \frac{1}{3}\nu_m kTb^2 \times \left[-\frac{1}{2a_x^2}\langle\hat{\mathbf{x}}\hat{\mathbf{x}}\rangle - \frac{1}{2a_y^2}\langle\hat{\mathbf{y}}\hat{\mathbf{y}}\rangle + \left(\frac{1}{a_x^2} + \frac{1}{a_y^2}\right)\langle\hat{\mathbf{z}}\hat{\mathbf{z}}\rangle\right] \tag{A4}$$

where the ensemble average is preserved only over the unit vectors, two of which are not constant in the biaxial case (see below).

Equation A3 was derived under the assumption that chains are equilibrated within their tubes, which applies to the present case as well. Notice also that one positive and two negative terms appear in the expression, corresponding to traction along the tube axis and compression on the tube wall, respectively. Positive and negative terms are complete with their respective numerical coefficients, as they emerge from the equilibrium theory. We now specialize eq A4 for the three different elongational flows.

Uniaxial. In this case the unit vectors are constant in the ensemble, and because of the uniaxial symmetry, it is $a_x = a_y = a$. Therefore, the single nonzero normal stress difference σ is obtained from eq A4 as

$$\sigma_{\text{uniaxial}} = T_{zz} - T_{xx} = \frac{5}{6}\nu_m kT\,\frac{b^2}{a^2} \tag{A5}$$

Planar. Also in this case the unit vectors are constant in the ensemble, and we elect $\hat{\mathbf{x}}$ to lie in the compressive direction, where the tube size $a_x = a$ is smallest. In the neutral direction, along which there is neither compression nor traction, we will assume $a_y = a_0$. The normal stress difference that is usually measured is that between the traction and the compression directions (the same of the inequality A1). Hence, from eq A4 we obtain

$$\sigma_{\text{planar}} = T_{zz} - T_{xx} = \frac{1}{2}\nu_m kT\,\frac{b^2}{a^2}\left(1 + \frac{2}{3}\frac{a^2}{a_0^2}\right) \cong \frac{1}{2}\nu_m kT\,\frac{b^2}{a^2} \tag{A6}$$

where the latter approximate equality holds true for the case of interest here, i.e., when a^2 is much smaller than the equilibrium value.

Equibiaxial. In this case, only the compressive direction ($\hat{\mathbf{x}}$, say) is constant in the ensemble, while $\hat{\mathbf{y}}$ and $\hat{\mathbf{z}}$ are uniformly distributed in the elongational plane. Hence, we need to calculate the averages $\langle\hat{\mathbf{y}}\hat{\mathbf{y}}\rangle$ and $\langle\hat{\mathbf{z}}\hat{\mathbf{z}}\rangle$. If $\hat{\mathbf{v}}$ and $\hat{\mathbf{w}}$ are mutually orthogonal unit vectors *fixed* in the elongational plane, we readily obtain

$$\langle \hat{\mathbf{y}}\hat{\mathbf{y}} \rangle = \langle \hat{\mathbf{z}}\hat{\mathbf{z}} \rangle = \frac{1}{2}\hat{\mathbf{v}}\hat{\mathbf{v}} + \frac{1}{2}\hat{\mathbf{w}}\hat{\mathbf{w}} \tag{A7}$$

so that eq A4 becomes in this case:

$$\mathbf{T} = \frac{1}{3}\nu_m kTb^2\left[-\frac{1}{2a_x^2}\hat{\mathbf{x}}\hat{\mathbf{x}} + \left(\frac{1}{2a_x^2} + \frac{1}{4a_y^2}\right)\hat{\mathbf{v}}\hat{\mathbf{v}} + \left(\frac{1}{2a_x^2} + \frac{1}{4a_y^2}\right)\hat{\mathbf{w}}\hat{\mathbf{w}}\right] \tag{A8}$$

The nonzero normal stress difference is obtained as

$$\sigma_{\text{biaxial}} = T_{ww} - T_{xx} = \frac{1}{3}\nu_m kT\frac{b^2}{a^2}\left(1 + \frac{a^2}{4a_y^2}\right) \cong \frac{1}{3}\nu_m kT\frac{b^2}{a^2} \tag{A9}$$

where, as before, we have set the smallest tube dimension $a_x = a$, and the approximate equality holds true (when a^2 becomes much smaller than the equilibrium value) because, as mentioned above, it is likely that traction in the y-direction makes a_y even larger than a_0.

The values of σ in eqs A5, A6, and A9 show the correct ordering as in the inequality A1 if the comparison is made at equal values of a. However, the crucial comparison is to be made at equal values of $\dot{\epsilon}$. Hence, we proceed as follows. Accounting for numerical coefficients, we rewrite the steady-state force balance of eq 9 that determines the compressive dimension a of the tube in each type of flow. In fact, if the unknown influence of CCR is neglected altogether, we can write a single equation for all three cases:

$$\frac{1}{6}kTNb^2\left(\frac{1}{a^3} - \frac{1}{a_0^3}\right) = \zeta|\dot{a}_{\text{affine}}| \tag{A10}$$

Here, the $\dot{a}_{\text{affine}}$ term is of course different in the three cases, whereas the $^1/_6$ factor of the compressive force is the same for all of them. Indeed, in the previous expressions for the stress tensor, the coefficient in the compressive x-direction is always the same and equal to $\nu_m kTb^2/6a^2$. Now, since the number of chains in a slab of unit area and thickness a is equal to νa in all cases as well, there follows that the compressive force is given by $NkTb^2/6a^3$in all three types of elongational flows.

By using for $|\dot{a}_{\text{affine}}|$ the expressions $\dot{\epsilon}a/2$, $\dot{\epsilon}a$, and $2\dot{\epsilon}a$ for the uniaxial, planar, and equibiaxial case, respectively, we obtain from eq A10 the following power laws:

$$a_{\text{uniaxial}} = \left(\frac{kTNb^2}{3\zeta\dot{\epsilon}}\right)^{1/4}; \quad a_{\text{planar}} = \left(\frac{kTNb^2}{6\zeta\dot{\epsilon}}\right)^{1/4}; \quad a_{\text{equibiaxial}} = \left(\frac{kTNb^2}{12\zeta\dot{\epsilon}}\right)^{1/4} \tag{A11}$$

Finally, these expressions are replaced in eqs A5, A6, and A9, respectively, to yield

$$\sigma_{\text{uniaxial}} = \frac{5}{6}\nu_m(3kTb^2\zeta_m\dot{\epsilon})^{1/2}$$

$$\sigma_{\text{planar}} = \frac{\sqrt{2}}{2}\nu_m(3kTb^2\zeta_m\dot{\epsilon})^{1/2}$$

$$\sigma_{\text{equibiaxial}} = \frac{2}{3}\nu_m(3kTb^2\zeta_m\dot{\epsilon})^{1/2} \tag{A12}$$

where, since it is $5/6 > 1/\sqrt{2} > 2/3$, the correct ordering of eq A1 is reproduced.

References and Notes

(1) Doi, M.; Edwards, S. F. *The Theory of Polymer Dynamics*; Clarendon: New York, 1986.
(2) de Gennes, P. G. *J. Chem. Phys.* **1971**, *55*, 572.
(3) Doi, M. *J. Polym. Sci., Polym. Lett. Ed.* **1981**, *19*, 265.
(4) Graessley, W. W. *Adv. Polym. Sci.* **1982**, *47*, 67.
(5) Marrucci, G.; Grizzuti, N. *Gazz. Chim. It.* **1988**, *118*, 179.
(6) Marrucci, G. *J. Non-Newtonian Fluid Mech.* **1996**, *62*, 279.
(7) Ianniruberto, G.; Marrucci, G. *J. Non-Newtonian Fluid Mech.* **1996**, *65*, 241.
(8) Mead, D. W.; Larson, R. G.; Doi, M. *Macromolecules* **1998**, *31*, 7895.
(9) Öttinger, H. C. *J. Rheol.* **1999**, *43*, 1461.
(10) Marrucci, G.; Ianniruberto, G. *Philos. Trans. R. Soc. London, A* **2003**, *361*, 677.
(11) Graham, R. S.; Likhtman, A. E.; McLeish, T. C. B.; Milner, S. T. *J. Rheol.* **2003**, *47*, 1171.
(12) Bent, J.; Hutchings, L. R.; Richards, R. W.; Gough, T.; Spares, R.; Coates, P. D.; Grillo, I.; Harlen, O. G.; Read, D. J.; Graham, R. S.; Likhtman, A. E.; Groves, D. J.; Nicholson, T. M.; McLeish, T. C. B. *Science* **2003**, *301*, 1691.
(13) Marrucci, G.; de Cindio, B. *Rheol. Acta* **1980**, *19*, 68.
(14) Marrucci, G.; Hermans, J. J. *Macromolecules* **1980**, *13*, 380.
(15) Wagner, M. H.; Schaeffer, J. *J. Rheol.* **1992**, *32*, 1.
(16) Wagner, M. H.; Rubio, P.; Bastian, H. *J. Rheol.* **2001**, *45*, 1387.
(17) Archer, L. A.; Mhetar, V. R. *Rheol. Acta* **1998**, *37*, 170.
(18) Rubinstein, M.; Panyukov, S. *Macromolecules* **2002**, *35*, 6670.
(19) Bach, A.; Almdal, K.; Rasmussen, H. K.; Hassager, O. *Macromolecules* **2003**, *36*, 5174.
(20) Bhattacharjee, P. K.; Oberhauser, J. P.; McKinley, G. H.; Leal, L. G.; Sridhar, T. *Macromolecules* **2002**, *35*,10131.
(21) Bhattacharjee, P. K.; Nguyen, D. A.; McKinley, G. H.; Sridhar, T. *J. Rheol.* **2003**, *47*, 269.
(22) Ye, X.; Larson, R. G.; Pattamaprom, C.; Sridhar, T. *J. Rheol.* **2003**, *47*, 443.
(23) This formula is reported as eq (2.66) at p 20 of the Doi−Edwards book.[1]
(24) Leonardi, F.; Majeste, J. C.; Allal, A.; Marin, G. *J. Rheol.* **2000**, *44*, 675.
(25) Ferry, J. D. *Viscoelastic Properties of Polymers*; Wiley: New York, 1980.
(26) Kroger, M.; Hess, S. *Phys. Rev. Lett.* **2000**, *85*,1128.
(27) Smith, G. D.; Paul, W.; Monkenbusch, M.; Richter, D. *J. Chem. Phys.* **2001**, *114*, 4285.
(28) Kreer, T.; Baschnagel, J.; Mueller, M.; Binder, K. *Macromolecules* **2001**, *34*, 1105.
(29) Padding, J. T.; Briels, W. J. *J. Chem. Phys.* **2001**, *115*, 2846.
(30) Padding, J. T.; Briels, W. J. *J. Chem. Phys.* **2002**, *117*, 925.
(31) Colby, R. H.; Fetters, L. J.; Graessley, W. W. *Macromolecules* **1987**, *20*, 2226.
(32) Gray, R. W.; Harrison, G.; Lamb, J. *Proc. R. Soc. London, A* **1977**, *356*, 77.
(33) Moore, J. D.; Cui, S. T.; Cochran, H. D.; Cummings, P. T. *Phys. Rev. E* **1999**, *60*, 6956.
(34) Padding, J. T.; Briels, W. J. *J. Chem. Phys.* **2003**, *118*, 10276.
(35) During the Spring 2002 program on Dynamics of Complex and Macromolecular Fluids at the Kavli Institute for Theoretical Physics in Santa Barbara, CA, a discussion involving many participants addressed the observed differences in $G''(\omega)$ between melts and solutions. Concentration fluctuations, which are absent in melts, were indicated as a possible explanation.
(36) Ianniruberto, G.; Marrucci, G. *J. Non-Newtonian Fluid Mech.* **1998**, *79*, 225.
(37) Sanchez-Reyes, J.; Archer, L. A. *Macromolecules* **2002**, *35*, 5194.
(38) Archer, L. A.; Sanchez-Reyes, J.; Juliani *Macromolecules* **2002**, *35*, 10216.
(39) Meissner, J.; Stephenson, S. E.; Demarmels, A.; Portmann, P. *J. Non-Newtonian Fluid Mech.* **1982**, *11*, 221.
(40) Hachmann, P.; Meissner, J. *J. Rheol.* **2003**, *47*, 989.

MA035501U